

Bohmian description of a decaying quantum system

Y. Nogami^a, F.M. Toyama^b, W. van Dijk^{a,c,1}

^a*Department of Physics and Astronomy, McMaster University, Hamilton,
Ontario, Canada L8S 4M1*

^b*Department of Communication and Information Sciences, Kyoto Sangyo
University, Kyoto 603-8555, Japan*

^c*Redeemer College, Ancaster, Ontario, Canada L9K 1J4*

Abstract

We present a Bohmian description of a decaying quantum system. A particle is initially confined in a region around the origin which is surrounded by a repulsive potential barrier. The particle leaks out in time tunneling through the barrier. We determine Bohm trajectories with which we can visualize various features of the decaying system.

Key words: Bohm trajectories, α -decay

1 Introduction

Consider a nonrelativistic particle in a given potential field. In Bohm's ontological interpretation of quantum mechanics, the position and velocity of the particle are both well-defined at any instant of time. The particle moves along a Bohm trajectory, irrespective of whether or not the particle is observed [1–4]. The Schrödinger wave function accompanies and guides the particle [5]. We do not talk about the collapse of the wave function caused by observation. A certain "surrealistic" aspect of the Bohm trajectory in the presence of a Welcher Weg (which way) detector has been discussed recently but we do not consider such a situation in this Letter [6].

The particle obeys Newton's equation of motion with a potential which consists of the usual given potential and the "quantum potential". The latter is

¹ E-mail: vandijk@physics.mcmaster.ca

related to the amplitude of the wave function. The initial condition of the motion, however, can be determined only statistically. With this statistical uncertainty implemented, Bohm's theory agrees with the traditional quantum mechanics for all observable quantities. But the picture that Bohm's theory offers is strikingly different from the traditional one. A variety of problems have been examined on the basis of Bohm's theory. Among them let us mention the recent work by Leavens et al. and Oriols et al. [7,8] on the one-dimensional tunneling problem, which has direct relevance to what we propose to examine. The purpose of this Letter is to extend the application of Bohm's theory to the decay problem.

We consider a model with a particle in a central potential $V(r)$. The potential has a repulsive barrier that supports one or more unstable bound states or resonances. The particle is initially confined inside the potential barrier and at a certain time, $t = 0$, it begins to leak out. The model and its variants can be used to simulate a decay process through tunneling such as the nuclear α decay [9] or the emission of an electron from an artificial atom (quantum dot) [10]. In order to apply Bohm's theory to such a system, one has to know the wave function of the system explicitly. Bohm's approach has not been attempted for the decay problem so far. This is because very little has been known about the wave function of such a decaying system, particularly outside the potential barrier. A recently developed technique, however, has made it possible to solve the time-dependent Schrödinger equation accurately, at least for the type of model that we consider below, no matter how large r and t are [11].

In Section 2 we set up the model and we present a solution of the time-dependent Schrödinger equation of the model with an appropriate initial condition. In Section 3 we work out the Bohmian description of the decay process and discuss various features such as the exponential decay law and deviation from it at very small time. A summary is given in Section 4.

2 Model

We assume a simple model with the repulsive potential barrier,

$$V(r) = (\lambda/a)\delta(r - a), \quad (1)$$

where $\lambda > 0$ and $a > 0$ are constants. A particle is initially confined inside the potential barrier and it begins to leak out at $t = 0$. This model has been used by a number of authors to examine various features of the decaying quantum system such as the exponential decay law and deviations from it at very small

time as well as at very large time [12–14]. We use units such that $\hbar = 1$ and $2m = 1$ where m is the mass of the particle of the model. In numerical illustrations we set $a = 1$. For the strength of the potential we take $\lambda = 6$, which is one of the cases assumed in earlier work [12,14]. The λ corresponds to the G of [14].

We consider only the S state. The wave function $\psi(r, t)$ (actually the wave function times r) is determined by the time-dependent Schrödinger equation for $t > 0$,

$$i\frac{\partial\psi(r, t)}{\partial t} = \left[-\frac{\partial^2}{\partial r^2} + V(r)\right]\psi(r, t), \quad \psi(0, t) = 0. \quad (2)$$

For the initial condition for $\psi(r, t)$, let us assume the normalized function

$$\psi(r, 0) = \sqrt{\frac{2}{a}} \sin\left(\frac{\pi r}{a}\right) \theta(a - r), \quad (3)$$

where $\theta(x) = 1$ (0) if $x > 0$ ($x < 0$).

Although the model is very simple, its time-dependent Schrödinger equation is nontrivial to solve [12]. The wave function of the model in the entire space was found in an analytical form only recently [11]. It reads as

$$\psi(r, t) = \sum_{\nu} c_{\nu} [M(k_{\nu}, r - a, t) + N_{-}(k_{\nu}, r - a, t)], \quad (4)$$

$$N_{\pm}(k, x, t) = \frac{i\lambda}{2ka} [M(k, x, t) \pm M(k, -x, t)] \theta(-x), \quad (5)$$

where the summation is over $\nu = \pm 1, \pm 2, \dots$. The k_{ν} 's, which are determined by solving the equation $ka \cot ka + \lambda - ika = 0$ for k , are the positions of the poles of the S matrix. They are all in the lower half of the complex k plane. We designate the poles in the fourth (third) quadrant with $\nu = 1, 2, \dots$ ($\nu = -1, -2, \dots$). For $r > a$, $c_{\nu} = -2\pi i a_{\nu}(r) e^{ik_{\nu}a}$ for the $a_{\nu}(r)$ defined in [11]. It is given by

$$c_{\nu} = \frac{2\pi\sqrt{2a}k_{\nu}}{(k_{\nu}^2 a^2 - \pi^2)[(1 + \lambda - ik_{\nu}a) \cot k_{\nu}a - i - k_{\nu}a]}. \quad (6)$$

The c_{ν} 's satisfy $\sum_{\nu} c_{\nu}/k_{\nu} = 0$, but $\sum_{\nu} c_{\nu} \neq 0$. The $M(k, x, t)$ is the Moshinsky function [15]

$$M(k, x, t) = \frac{1}{2} e^{-ik^2 t} e^{ikx} \operatorname{erfc}(y), \quad y = e^{-i\pi/4} \left(\frac{x - 2kt}{2\sqrt{t}} \right), \quad (7)$$

where $\text{erfc}(y) = (2/\sqrt{\pi}) \int_y^\infty e^{-u^2} du$. In the limit of $t \rightarrow 0$, $M(k, x, t)$ becomes discontinuous at $x = 0$. Otherwise $M(k, x, t)$ is a smooth function of x . The $\psi(r, t)$ for $t > 0$ is continuous at $r = a$ as can be seen from $N_-(k, 0, t) = 0$.

The r -derivatives of $\psi(r, t)$ are given by

$$\begin{aligned} \psi'(r, t) = & i \sum_{\nu} c_{\nu} \{ k_{\nu} [M(k_{\nu}, r - a, t) \\ & + N_+(k_{\nu}, r - a, t)] + \chi(r - a, t) \}, \end{aligned} \quad (8)$$

$$\begin{aligned} \psi''(r, t) = & \sum_{\nu} c_{\nu} \{ -k_{\nu}^2 [M(k_{\nu}, r - a, t) + N_-(k_{\nu}, r - a, t)] \\ & + \frac{r - a + 2k_{\nu}t}{2t} \chi(r - a, t) \} + \frac{\lambda}{a} \delta(r - a) \psi(a, t), \end{aligned} \quad (9)$$

$$\chi(x, t) = \frac{e^{i\pi/4}}{2\sqrt{\pi t}} \exp\left(\frac{ix^2}{4t}\right). \quad (10)$$

It is not difficult to confirm that ψ of Eq. (4) does satisfy Eq. (2). The δ -function part of ψ'' exactly cancels $V\psi$ in the Schrödinger equation. In deriving ψ , ψ' and ψ'' we used $\sum_{\nu} c_{\nu}/k_{\nu} = 0$. The convergence of the ν summation for ψ can be dramatically improved by adding $\chi(r - a, t) \sum_{\nu} c_{\nu}/k_{\nu}$, which is formally zero, to the right hand side of Eq. (4).

3 Bohmian description

We write the wave function as

$$\psi(r, t) = R(r, t) \exp[iS(r, t)], \quad (11)$$

where $R(r, t)$ and $S(r, t)$ are both real. Then Eq. (2) leads to

$$\frac{\partial S}{\partial t} + (S')^2 + U(r, t) = 0, \quad (12)$$

$$U(r, t) = V(r) + Q(r, t), \quad Q(r, t) = -R''/R, \quad (13)$$

$$\frac{\partial R^2}{\partial t} + 2(R^2 S')' = 0, \quad (14)$$

where $S' = \partial S/\partial r$ and $R'' = \partial^2 R/\partial r^2$. The $Q(r, t)$ is the quantum potential.

In Bohm's interpretation, the particle obeys Newton's equation of motion with the potential $U(r, t) = V(r) + Q(r, t)$. Equation (12) is the classical Hamilton-Jacobi equation with potential $U(r, t)$. The momentum $p = mv$ ($m = 1/2$) of the particle at (r, t) is given by

$$p = mv = S'(r, t). \quad (15)$$

This p should not be confused with the usual quantum momentum operator. Equation (15) together with an appropriate initial condition determines the particle trajectory. The motion is causal and deterministic. The underlying potential $U(r, t)$ is of a nonlocal and holistic nature. It depends on the wave function which in turn is related to aspects of the system at points different from r .

The motion is subject to uncertainty in the sense that the initial condition is known only statistically. The particle may start at any point $r = r_0$ within the potential barrier; $0 < r_0 < a$. Since $S(r, 0) = 0$ for the $\psi(r, 0)$ of Eq. (3), the initial velocity is zero, i.e., $v(r_0, 0) = 0$. Two trajectories starting at different points at $t = 0$ do not cross each other [2,7,8]². It is understood that the probability with which the particle starts at r_0 is proportional to $|\psi(r_0, 0)|^2$. An observable quantity of the system is calculated by taking an average over all possible trajectories weighted according to $|\psi(r_0, 0)|^2$. Equation (14) guarantees the conservation of the probability of the particle in the statistical ensemble of the trajectories.

With the wave function given in Section 2 we can determine R , S and their derivatives by using $\text{Im}(\psi'/\psi) = S'$, $\text{Re}(\psi''/\psi) = (R''/R) - S'^2$, etc. At $r = a$, it can be shown that R , S and S' are all continuous, while $R'(a+0, t) - R'(a-0, t) = (\lambda/a)R(a, t)$. The quantum potential Q contains a δ -function term, which cancels the δ -function of V in potential U . When $t > 0$, U is continuous at $r = a$. At $t = 0$, we have

$$Q(r, 0) = \left(\frac{\pi}{a}\right)^2, \quad r < a. \quad (16)$$

Unlike for $t > 0$, there is no exact cancellation of the δ -function terms of Q and V at $t = 0$ and hence $U(r, 0)$ is singular at $r = a$. As soon as t becomes positive, this singularity disappears. Let us define the energy $E(r, t)$ of the particle by

$$E(r, t) = p^2 + U(r, t). \quad (17)$$

² Since we are considering only the S state the wave function is independent of angles. The velocity associated with a Bohm trajectory has only a radial component. The particle that starts at r_0 moves always in the radial direction. In this Letter by a trajectory we mean a plot of r versus t , not a path in the xyz configuration space.

The particle can start at any point $0 < r_0 < a$. Since $v(r_0, 0) = 0$, the initial value of the energy is $E(r_0, 0) = (\pi/a)^2$ which is independent of r_0 . Note, however, $E(r, t)$ is not conserved during the motion because $U(r, t)$ depends on t explicitly.

The trajectories can be labeled in terms of the starting point r_0 . Instead of r_0 , it is often more convenient to use

$$s(r_0) = \int_0^{r_0} \psi^2(r, 0) dr = \frac{r_0}{a} - \frac{1}{2\pi} \sin\left(\frac{2\pi r_0}{a}\right), \quad (18)$$

which is the probability for the particle being in the region $(0, r_0)$ at $t = 0$. Note that $s(a) = 1$, $s(a/2) = 1/2$ and $s(0) = 0$. For the trajectory that starts at r_0 at $t = 0$, let us denote the position function with $r(r_0, t)$. We determine $r(r_0, t)$ by solving Eq. (15). The consistency between the trajectory and the wave function requires that

$$s(r_0) = \int_0^{r(r_0, t)} |\psi(r, t)|^2 dr, \quad (19)$$

at any time. This is based on the noncrossing nature of the trajectories. In fact, Eq. (19) can be used as an alternative method of determining $r(r_0, t)$ [8]. We have numerically solved Eq. (15) starting with a small but finite value of t , in order to avoid the highly oscillatory behavior of $\psi(r, t)$ as $t \rightarrow 0$. We have verified our solutions by varying the initial value of t and also by using Eq. (19).

So far we have assumed that the trajectories start at $t = 0$. We will assume the same in the rest of this Letter unless we state otherwise. Let us note, however, that the starting time can be chosen at will. For a trajectory that starts at position r and time $t > 0$ with velocity $S'(r, t)$, one can unambiguously trace its history back to $t = 0$. We will do this later for the trajectories shown in Fig. 4.

The quantum decay process generally goes through three stages, I, II and III, which are characterized by different t dependence of the nonescape probability $P(t)$ [12,16],

$$P(t) = \int_0^a |\psi(r, t)|^2 dr. \quad (20)$$

In the initial stage I we have, approximately, $1 - P(t) \propto t^2$. We have the exponential law $P(t) = e^{-\Gamma t}$ in stage II and the power law $P(t) \propto 1/t^3$ in final

stage III [17,18]³.

Between the three stages are transition periods in which $P(t)$ exhibits an irregular, oscillatory behaviour [12]. Stage II usually spans most of the life time of the decaying system. In our model with the chosen parameters the transition between stages I and II is around $t = 0.2$ and that between II and III is around $t = 12$. Toward the end of stage II, $P(t)$ becomes as small as 10^{-8} . By then the system has almost completely decayed. We present results in five figures.

In Fig. 1 we show trajectories with equally spaced s , with interval of $\Delta s = 1/N$, $N = 30$. These trajectories have equal statistical weights. In other words, each of the trajectories occurs with the same probability. The trajectory density at (r, t) is proportional to the probability density $|\psi(r, t)|^2$. The trajectories do not cross each other. A trajectory that starts near the barrier ($a = 1$) escapes earlier. Outside the barrier the trajectories become nearly straight. The slopes of the four or five trajectories that leave the barrier the earliest are somewhat steeper than the others. If we assume that $E(r, t)$ of Eq. (17) is conserved and that $U(r, t)$ is negligible for $r > a$, we obtain $E(r, t) = Q(r, 0) = (\pi/a)^2$ for $r > a$. This leads to $p = \pi/a$ and $v = 2\pi$ ($2m = 1$, $a = 1$) outside the barrier. This is approximately the case as can be seen from the slopes of the trajectories of Fig. 1.

Let us label the trajectories with $n = 1, 2, \dots, 29$, starting with the one that escapes first. In terms of the starting point r_0 , trajectory 1 is the closest to the barrier. For each of the trajectories we define the escape time t_n as the time at which the particle crosses $a = 1$ outward. (Such escape times or “exit times” have been formally discussed by Daumer et al. [19] in the context of the scattering problem in three dimensions.) At $t = t_n$ out of the N trajectories, $(N - n)$ trajectories are still within the boundary. This means that the nonescape probability $P(t)$ is given by

$$P(t) = \frac{N - n}{N}, \quad t_n < t < t_{n+1}. \quad (21)$$

Ideally N should be taken as an infinitely large number. If the exponential decay law holds exactly, that is, if $P(t) = e^{-\Gamma t}$, we obtain

$$t_n = \frac{1}{\Gamma} \ln \left(\frac{N}{N - n} \right), \quad (22)$$

³ There is a claim that $P(t) \propto 1/t$ in stage III [17]. On the other hand it was argued that it is $1/t^3$ [18]. For our model we can calculate $P(t)$ directly by using the explicit wave function of Eq. (4). We find that $P(t) \propto 1/t^3$ in stage III, in agreement with [18].

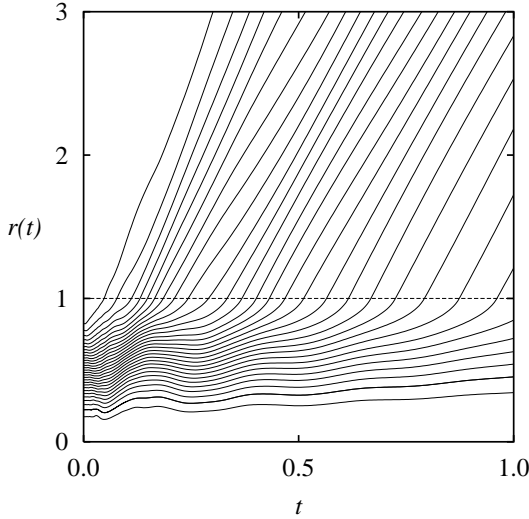


Fig. 1. Bohm trajectories (with $\lambda = 6$) with equally spaced s of Eq. (18), with interval of $\Delta s = 1/30$. These trajectories have equal statistical weight. The trajectory density at (r, t) is proportional to the probability density $|\psi(r, t)|^2$. The units are such that $\hbar = 1$, $2m = 1$ and $a = 1$.

where Γ is related to the half-life $\tau_{1/2}$ through $\tau_{1/2} = \ln 2/\Gamma$. Figure 2 shows t_n versus $\ln[N/(N-n)]$. The dots correspond to the trajectories shown in Fig. 1.

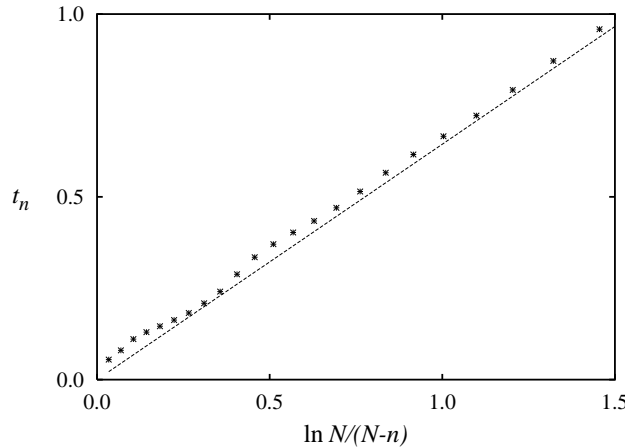


Fig. 2. The escape time, at which the particle crosses the barrier at $r = a = 1$ outward. The dots correspond to the trajectories of Fig. 1. They are labeled with $n = 1, 2, \dots$, starting with the one that escapes first. The dotted line is based on the exponential decay law, with $1/\Gamma = 0.644$. The parameters of the model and units are the same as in Fig. 1.

By fitting the numerically calculated nonescape probability of the same model as ours with $P(t) = e^{-\Gamma t}$, Winter obtained $1/\Gamma = 0.644$ which leads to $\tau_{1/2} = 0.446$ [12]. In Fig. 2 the dashed line shows the n dependence of t_n given by

Eq. (22) with Winter's $1/\Gamma$. Except for the first several ones, the dots follow the exponential curve very well. The 15-th trajectory starts at $r_0 = 0.5$ and $s = 0.5$. It crosses the barrier at $t_{15} = 0.468$, which is the half-life $\tau_{1/2}$. This is slightly larger than the value 0.446 which is based on Winter's estimate. (In Section 3 of [14] below Eq. (17) the half-life for $G = 6$ was misquoted as $\tau_{1/2} = 1.08$. The correct value is 0.446.) Note that the decay process begins at a rate slower than predicted by the exponential law. This explains why the $\tau_{1/2}$ estimated by the trajectory of $s = 1/2$ is greater than the one based on the exponential law.

For $t < 0.2$ the escape time does not follow the exponential law very well. It is in fact better fitted with $t_n \propto \sqrt{n}$. In Fig. 3 we plot the escape time against \sqrt{n} . In order to see the details we have increased the number of trajectories, which are again equally spaced with respect to s but with a smaller interval $\Delta s = 1/N$ with $N = 100$. They are labelled with $n = 1, 2, \dots, 99$ but the escape time is shown only for the first 25 trajectories. The first three dots are almost exactly on a straight line which passes through the origin. This means that $1 - P(t) \propto t^2$ and hence $dP(t)/dt = 0$ at $t = 0$. In the beginning of the decay process, $P(t)$ decreases more slowly than the exponential law predicts. This is analogous to the “standby mechanism” which Elberfeld and Kleber [20] discussed in their analysis of time-dependent tunneling of a semi-infinite wave train through a thin barrier. This deviation from the exponential law for very small t is a general feature of the quantum decay process which is related to the possibility of the quantum Zeno effect as discussed in [16]. For experimental evidence, see [21].

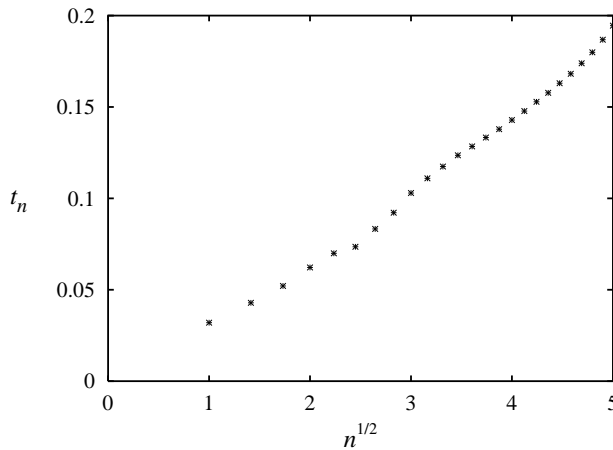


Fig. 3. The escape times at very small times. In this case $N = 100$ and t_n is plotted against \sqrt{n} . The parameters of the model and units are the same as in Fig. 1.

Let us take the model as a simulation of an α -decaying nucleus and examine how the nuclear charge $Z(t)$ (in units of $e > 0$) varies as a function of t when

the α particle of charge 2 is emitted. In the traditional theory the charge number $Z(t)$ of the nucleus is given by

$$Z(t) = Z(0) - 2[1 - P(t)]. \quad (23)$$

The nonescape probability is well approximated by $P(t) = e^{-\Gamma t}$ for most of the time. The $Z(t)$ changes from $Z(0)$ to $Z(0) - 2$ gradually. This is because the wave function $\psi(r, t)$ of the α particle leaks out gradually.

In the Bohmian description, if one follows the n -th trajectory, the nuclear charge changes from $Z(0)$ to $Z(0) - 2$ suddenly at time t_n when the α particle leaves the nucleus and hence

$$Z_n(t) = Z(0) - 2\theta(t - t_n). \quad (24)$$

Here suffix n refers to the n -th trajectory. In order to obtain the nuclear charge that can be compared with that of the traditional theory, we have to consider the ensemble of all trajectories each with a weight $|\psi(r_0, 0)|^2$. This weight in the present case is $1/N$ for each trajectory. At time t such that $t_n < t < t_{n+1}$, the particles of trajectories of $1, 2, \dots, n$ have escaped. We thus obtain

$$Z(t) = Z(0) - \frac{2n}{N} = Z(0) - 2[1 - P(t_n)], \quad (25)$$

where we have used Eq. (21). In the limit of $N \rightarrow \infty$, this $Z(t)$ converges to the $Z(t)$ of Eq. (23) of the traditional theory. This illustrates how a quantity that appears in the Bohmian description can be related to its counterpart of the traditional theory.

Consider a gedanken experiment in which one tries to detect an α particle that is emitted from a source consisting of a single α emitting nucleus. The event in which one detects an α particle corresponds to one of the Bohm trajectories. If one repeats this experiment many times one experiences events, each of which is described by one of the Bohm trajectories. Here it is understood that the source is prepared every time in an identical manner. In contrast to this, the Schrödinger wave function does not describe any of the individual events, rather it only describes an ensemble of a large number of such events. Instead of repeating the experiment on one system, we can think of experiments on many independent systems that are all identically prepared. In this sense, the word “event(s)” can be replaced with “system(s)”.

Figure 4 shows 21 trajectories such that $r(t = 10)$ ranges from 0.2 to 0.6 with the interval $\Delta r = 0.02$. We have obtained these trajectories by integrating Eq. (15) starting at $t = 10$. For the starting points, we have chosen to keep

Δr constant rather than Δs . This choice is only a matter of convenience or simplicity of the calculation involved. Because of this choice, unlike in Fig. 1, the trajectory density in this figure is not proportional to the probability density. For example, in the figure the statistical weight is larger for a trajectory with a larger value of $r(t = 10)$. The range in terms of probability $s(r_0)$ is from 6.44×10^{-9} to 1.047×10^{-7} . As we stated before we can easily trace the history of the trajectories back to $t = 0$. The values of r_0 at $t = 0$ of the trajectories range from 9.93×10^{-4} to 2.52×10^{-3} . These trajectories are starting almost from the origin. This is why they remain inside for a very long time.

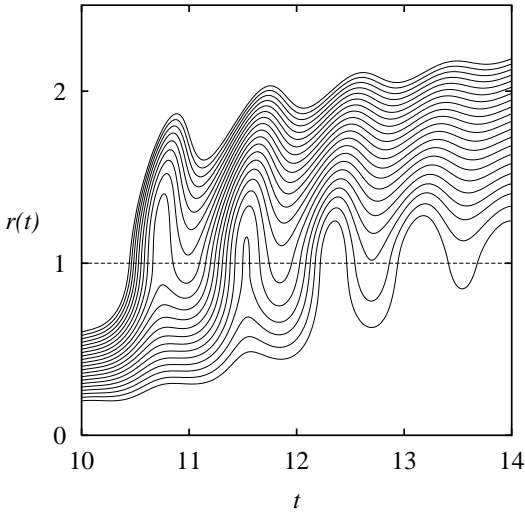


Fig. 4. Trajectories such that $r(t = 10)$ ranges from 0.2 to 0.6 with the interval $\Delta r = 0.02$. Because of this, unlike in Fig. 1, the trajectory density is not proportional to the probability density. The parameters of the model and units are the same as in Fig. 1.

The trajectories go back and forth across the barrier. As Winter pointed out many years ago, the current density $j(r, t)$ at the barrier fluctuates in this time interval [12,14]⁴. At times it becomes negative, i.e., inward. Figure 4 visualizes this feature. In such a situation we redefine the escape time as the time when the particle finally leaves the barrier. The exponential law does not hold in this time region any longer. Note also that, after leaking out through the potential barrier, the trajectories tend to remain close to the barrier. This situation is very different from that of Fig. 1. The time interval shown in Fig. 4 is the transition period between stages II and III. In the latter, the nonescape probability decreases like $1/t^3$.

Figure 5 shows the potential $U(r, t)$ which is equal to the quantum potential $Q(r, t)$ with its δ -function part removed. There is no potential barrier in $U(r, t)$

⁴ There are other space-time regions in which similar fluctuations (with larger amplitudes) of the current density occur. See Fig. 5 of [14].

and hence there is no tunneling phenomenon. As r increases across the barrier at $r = a = 1$, U sharply drops but U is continuous across the barrier (except at $t = 0$). The behavior of U is complicated for very small t and also for very small r . The figure does not show the part of $t < 0.05$ and $r < 0.001$. Close scrutiny reveals that the trajectories rapidly fluctuate when t and hence $r(t)$ are very small. Although we do not show it, the behavior of $U(r, t)$ is also complicated in the space-time region that corresponds to Fig. 4. For $r \gg a$, U becomes negligible.

The results shown above are all for the case of $\lambda = 6$. We have also examined the case of larger values of λ . For example, when $\lambda = 100$, the deviations from the exponential law are very small. Let us add that, if we are to simulate α decay processes, we have to assume much larger values of λ , for example, of the order of 10^8 for ^{212}Po . See Section 5 of [14].

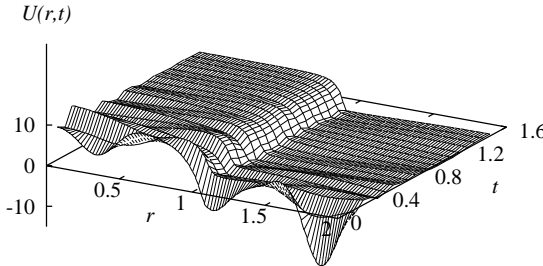


Fig. 5. Potential $U(r, t)$ which is equal to the quantum potential $Q(r, t)$ with its δ -function part removed. The U is continuous across the barrier $r = a (= 1)$ except at $t = 0$. The $U(r, t)$ for $r < 0.001$ and $t < 0.05$ are not shown. The parameters of the model and units are the same as in Fig. 1.

4 Summary

For the model defined by Eqs. (1) and (3) we examined the decay process from Bohm's point of view. We obtained Bohm trajectories with which we can interpret various features of the decay process. We see deviations from the exponential law at very small time and also at very large time. The decay process is slower in the beginning than the exponential law predicts. In the time interval of $t = 10$ to 14 , we showed that the trajectories go back and forth across the barrier. This corresponds to the current density fluctuations that Winter found. Beyond that time region, the exponential law is replaced

with a power law. One can verify this by showing that for large times and very small r_0 , $t_n \propto (N - n)^{-1/3}$, confirming that the trajectories in this region of very large time are consistent with $P(t) \propto 1/t^3$.

The results that we obtained in the Bohmian picture are complementary but not contradictory to the traditional quantum mechanics. Let us, however, emphasize the following point. In contrast to the Schrödinger wave function which describes an ensemble of a large number of events, each of the Bohm trajectories represents an individual event. Such information on individual events is masked when the uncertainty regarding the starting points of the trajectories is incorporated. In a situation in which one has to deal with an individual event, however, the Bohmian approach may lead to new insights.

The model that we have considered is one of the simplest models for the decay process. The method that we have used can be applied to other potential models.

Acknowledgements

This work was supported by the Natural Sciences and Engineering Research Council of Canada.

References

- [1] D. Bohm, Phys. Rev. 85 (1952) 166 and 180.
- [2] C. Philippidis, C. Dewdney, B.J. Hiley, Nuovo Cimento 52B (1979) 15; C. Dewdney, B.J. Hiley, Found. Phys. 12 (1982) 27.
- [3] D. Bohm, B.J. Hiley, Found. of Phys. 14 (1984) 255; D. Bohm, B.J. Hiley, P.N. Kaloyerou, Phys. Reports 144 (1987) 323; D. Bohm, B.J. Hiley, *The Undivided Universe: An Ontological Interpretation of Quantum Theory*, Routledge, London, 1993.
- [4] P.R. Holland, *The Quantum Theory of Motion*, Cambridge University Press, Cambridge, 1993.
- [5] L. de Broglie, Compt. Rend. Acad. Sci. Paris 183 (1926) 447; 184 (1927) 273; 185 (1927) 380.
- [6] B.-G. Englert, M.O. Scully, G. Süssmann, H. Walther, Z. Naturforsch. 47a (1992) 175; M.O. Scully, Phys. Scripta T76 (1998) 41; R.B. Griffiths, Phys. Lett. A 261 (1999) 227; Y. Aharonov, B.-G. Englert, M.O. Scully, Phys. Lett. A 263 (1999) 137.

- [7] C.R. Leavens, Solid State Commun. 74 (1990) 923; ibid 76 (1990) 253; Phys. Lett. A 197 (1995) 88; Phys. Rev. A 58 (1998) 840; C.R. Leavens, G.C. Aers, Scanning Tunneling Microscopy III, edited by Wiesendanger and H.-J. Güntherodt, Springer, New York, 1993, p. 105.
- [8] W.R. McKinnon, C.R. Leavens, Phys. Rev. A 51 (1995) 2478; X. Oriols, F. Martín, J. Suñé, Phys. Rev. A. 54 (1996) 2594.
- [9] G. Gamow, Z. Phys. 51 (1928) 204; E.U. Condon, R.W. Gurney, Nature 112 (1928) 439; Phys. Rev. 33 (1929) 127.
- [10] R.C. Ashoori, Nature 379 (1996) 413.
- [11] W. van Dijk, Y. Nogami, Phys. Rev. Lett. 83 (1999) 2867.
- [12] R.G. Winter, Phys. Rev. 123 (1961) 1503.
- [13] J. Petzold, Z. Phys. 155 (1959) 422; G. García-Caldéron, Symmetries of Physics, edited by A. Frank and K.B. Wolf, Springer, New York, 1992, p. 252; G. Garcí-Caldéron, G. Loyola, M. Moshinsky, ibid., p. 273.
- [14] W. van Dijk, F. Kataoka, Y. Nogami, J. Phys. A: Math. Gen. 32 (1999) 6347.
- [15] M. Moshinsky, Phys. Rev. 84 (1951) 525; 88 (1952) 625; H.M. Nussenzveig, Causality and Dispersion Relations, Academic Press, New York, 1972, Chap. 4.
- [16] B. Misra, E.C.G. Sudarshan, J. Math. Phys. 18 (1977) 756; C.B. Chiu, E.C.G. Sudarshan, B. Misra, Phys. Rev. D 16 (1977) 520; A. Peres, Am. J. Phys. 48 (1980) 931.
- [17] G. Garcí-Caldéron, J.L. Mateos, M. Moshinsky, Phys. Rev. Lett. 74 (1995) 337; 80 (1998) 4353.
- [18] R.M. Cavalcanti, Phys. Rev. Lett. 80 (1998) 5353.
- [19] M. Daumer, Bohmian Mechanics and Quantum Theory: An Appraisal, edited by J.T Cushing, A. Fine and S. Goldstein, Kluwer Academic Publishers, Boston, 1996, p. 87; M. Daumer, D. Dürr, S. Goldstein, N. Zanghi, J. Stat. Phys. 88 (1997) 967.
- [20] W. Elberfield, M. Kleber, Am. J. Phys. 56 (1988) 154.
- [21] S.R. Willkinson, C.F. Bharucha, M.C. Fisher, K.W. Madison, P.R. Morrow, Q. Niu, B. Sundaram, M.G. Raizen, Nature 387 (1997) 575.